Mechanism of the Phenylpyruvate Tautomerase Activity of Macrophage Migration Inhibitory Factor: Properties of the P1G, P1A, Y95F, and N97A Mutants[†,‡]

Stacy L. Stamps, Alexander B. Taylor, Susan C. Wang, Marvin L. Hackert, and Christian P. Whitman*

Department of Chemistry and Biochemistry, and the Medicinal Chemistry Division, College of Pharmacy, The University of Texas, Austin, Texas 78712-1074

Received February 16, 2000; Revised Manuscript Received May 11, 2000

ABSTRACT: Phenylpyruvate tautomerase (PPT) has been studied periodically since its activity was first described over forty years ago. In the last two years, the mechanism of PPT has been investigated more extensively because of the discovery that PPT is the same protein as the immunoregulatory cytokine known as macrophage migration inhibitory factor (MIF). The mechanism of PPT is likely to involve general base−general acid catalysis. While several lines of evidence implicate Pro-1 as the general base, the identity of the general acid remains unknown. Crystal structures of MIF with the competitive inhibitor (*E*)-2-fluoro-*p*-hydroxycinnamate bound in the active site and that of the protein complexed with the enol form of a substrate, (*p*-hydroxyphenyl)pyruvate, suggest that Tyr-95 is the only candidate in the vicinity that can function as a general acid catalyst. Although Tyr-95 is nearby the bound inhibitor and substrate, it is not within hydrogen bonding distance of either ligand. In this study, Tyr-95 was mutated to phenylalanine, and the kinetic and structural properties of the Y95F mutant were determined. This alteration produces a fully active enzyme, which shows no significant structural changes in the active site. The results indicate that Tyr-95 does not function as the general acid catalyst in the reaction catalyzed by wild-type PPT. The mechanism of PPT was studied further by constructing and characterizing the kinetic properties of two mutants of Pro-1 (P1G and P1A) and one mutant of Asn-97 (N97A). The mutation of Asn-97, a residue implicated in the binding of the phenolic hydroxy group of the keto and enol isomers of (*p*-hydroxyphenyl)pyruvate and of (*E*)-2-fluoro-*p*-hydroxycinnamate affects only the binding affinity of the inhibitor. However, the mutations of Pro-1 have a profound effect on the values of k_{cat} and k_{cat}/K_m and clearly show that Pro-1 is a critical residue in the reaction. The results are discussed in terms of a mechanism in which Pro-1 functions as both the general acid and the general base catalyst.

Phenylpyruvate tautomerase (PPT)[1] catalyzes the interconversion of the enol and keto isomers of phenylpyruvate (**1** → **2**, Scheme 1) and (*p*-hydroxyphenyl)pyruvate (**3** → **4**). Although this enzymatic activity was reported more than 40 years ago, its physiological significance remains unclear (*1*). In mammals, the enzyme is found in several tissues including the thyroid gland (*1*, *2*). Its location in the thyroid gland coupled with reports that PPT uses (diiodohydroxyphenyl)pyruvate as a substrate suggested that it might be involved in the thyroxine biosynthetic pathway (*2*). It is not known what role the enzymatic activity might play in the other mammalian tissues. PPT may also be part of the biosynthetic pathways for various alkaloids and other plant-derived bioactive substances, but specific substrates have not been identified (*3*, *4*).

Scheme 1

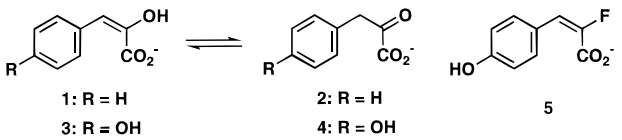

1: R = H **3: R = OH** **2: R = H** **4: R = OH** **5**

Recently, it was discovered that PPT is the same protein as a mammalian cytokine known as macrophage migration inhibitory factor (MIF) (*5*). MIF has been implicated in various immune and inflammatory processes and in the development of sepsis (*6*−*9*), adult respiratory distress syndrome (*10*), rheumatoid arthritis (*11*), and glomerulonephritis (*11*). Thus, it became of interest to determine whether there is a connection between the PPT activity and any of the biological activities of MIF, as PPT inhibitors might assist in the development of novel antiinflammatory agents (*12*−*15*). While a number of potential connections have been examined, an unequivocal link has not yet been established (*12*−*14*).

[†] This research was supported by Texas Advanced Research Program (ARP-183) to C.P.W. and the National Institutes of Health Grant GM-30105 and the Robert A. Welch Foundation (F-1219) to M.L.H.

[‡] The coordinates have been deposited with the Brookhaven Protein Data Bank (PDB code 1MFF).

* To whom correspondence should be addressed. Tel: 512-471-6198. Fax: 512-232-2606. E-mail: whitman@mail.utexas.edu.

[1] Abbreviations: ARP, automated refinement procedure; BCA, bicinchoninic acid; cc, correlation coefficient; CHMI, 5-(carboxymethyl)-2-hydroxymuconate isomerase; DEAE, diethylaminoethyl; DTT, dithiothreitol; ESI-MS, electrospray ionization mass spectrometry; F_o, F_c, observed and calculated structure factors, respectively; HPLC, high-pressure liquid chromatography; IPTG, isopropyl-β-D-thiogalactoside; Kn, kanamycin; LB, Luria-Bertani medium; MIF, macrophage migration inhibitory factor; NMR, nuclear magnetic resonance; 4-OT, 4-oxalocrotonate tautomerase; PPT, phenylpyruvate tautomerase; SDS−PAGE, sodium dodecyl sulfate−polyacrylamide gel electrophoresis.

10.1021/bi000373c CCC: $19.00
Published on Web 07/15/2000

The PPT activity of MIF has also generated interest because the protein shares substantial structural homology with two bacterial isomerases, 4-oxalocrotonate tautomerase (4-OT) and 5-(carboxymethyl)-2-hydroxymuconate isomerase (CHMI) (*16*). The structures of the three proteins are nearly superimposable (*16*, *17*). Both MIF and CHMI are trimers of identical subunits. The MIF subunit consists of 114 amino acids, whereas the CHMI subunit is made up of 125 amino acids. 4-OT is a hexamer, consisting of identical 62-amino acid monomers. The structural similarities were surprising because there is little sequence identity among these three proteins although they all have an amino-terminal proline. Pro-1 has since been identified as the general base catalyst in each reaction (*18*−*21*). In addition to Pro-1, it was anticipated that a general acid catalyst would be present in each protein as other nonmetal requiring isomerases use general acid−base catalysis (*19*, *22*). In 4-OT, Arg-39 and an ordered water molecule polarize the carbonyl group of the substrate (*23*−*25*). Superimposition of the 4-OT and CHMI crystal structures suggests that Arg-40 might act as the general acid catalyst in CHMI (*18*).

Although a general acid catalyst for the PPT activity of MIF has not been determined, Tyr-95 appeared to be a likely candidate because it occupied a similar position to Arg-39 in 4-OT (*15*). However, the crystal structures of MIF complexed with two different ligands show that the hydroxyl group of Tyr-95 is not likely to be within hydrogen-bonding distance of the carbonyl oxygen of **2** or **4** (*15*, *21*). One crystal structure of a MIF·**3** complex places the hydroxyl group of Tyr-95 4.0 Å from the C-2 hydroxyl group of **3** (*21*). A second crystal structure of MIF complexed with the competitive inhibitor (*E*)-2-fluoro-*p*-hydroxycinnamate (**5**, Scheme 1) shows that the hydroxyl group of Tyr-95 is located 3.6 Å from the fluorine of **5**. (*15*). While these observations argue that Tyr-95 is not the general acid catalyst, both crystal structures show that the general base catalyst, Pro-1, is also not within hydrogen-bonding distance of C-3. For this reason, it can be inferred that these active site residues are sufficiently mobile enabling Pro-1 and Tyr-95 to function as general base and general acid catalysts, respectively. Significantly, neither structure shows another functional group in the area that can act as a general acid catalyst (*15*, *21*).

To clarify the role of Tyr-95 in the PPT activity of MIF, it was changed to a phenylalanine and the resulting Y95F mutant was characterized by kinetic and crystallographic studies. The mutation has little effect on the kinetic parameters and on the structure, making it unlikely that Tyr-95 would function as the general acid catalyst. The mechanism of the PPT activity was further studied by changing Pro-1, the catalytic base, to a glycine and an alanine. These mutations have a significant detrimental effect on catalysis, underscoring the importance of Pro-1 in the reaction. Finally, Asn-97, an active site residue implicated in the binding of the phenolic hydroxy group of **3** and **4** (*21*), and in the binding of the hydroxyl group of **5** (*15*), was changed to an alanine. Characterization of the N97A mutant shows that while its kinetic parameters are comparable to those of wild type, there is a modest decrease in the binding affinity of **5**. Together, these studies suggest a mechanism for the PPT activity in which Pro-1 functions as both the general base and the general acid catalyst.

MATERIALS AND METHODS

Materials. All biochemicals were purchased from either Aldrich or Sigma Chemical Co. with the exceptions noted in the text. Ultrafiltration membranes (10 000 MW cutoff) were purchased from Amicon. The clone containing recombinant mouse MIF was obtained from Dr. Richard Bucala (The Picower Institute for Medical Research, Manhasset, NY). The composition of LB medium is described elsewhere (*26*). (*E*)-2-Fluoro-*p*-hydroxycinnamic acid (**5**) was synthesized following a literature procedure (*3*).

General Methods. High pressure liquid chromatography (HPLC) was performed on a Waters system using a Waters Protein Pak (DEAE-5PW) anion-exchange column. Protein concentrations were determined using either the commercially available bicinchoninic acid (BCA) protein assay kit (Pierce Chemical Co., Rockford, IL) or the method of Waddell (*27*). Protein was analyzed by sodium dodecyl sulfate−polyacrylamide gel electrophoresis (SDS−PAGE) under denaturing conditions on 17% gels (*28*). The PPT activity was monitored by following the ketonization of **1** at 288 nm and of **3** at 300 nm in 50 mM sodium phosphate buffer (pH 6.5) as described (*15*). Competitive inhibition of the PPT activity by **5** was carried out as described using **3** as the substrate (*15*). Kinetic data were obtained on a Hewlett-Packard 8452A Diode Array spectrophotometer. The reaction mixtures in the cuvettes were mixed by a stir/add cuvette mixer. The kinetic data were fitted by nonlinear regression data analysis using the Grafit program (Erithacus Software Ltd., Staines, U. K.) obtained from Sigma Chemical Co. DNA sequencing was done at the University of Texas (Austin) Sequencing Facility. Electrospray ionization mass spectra were acquired using a LCQ Finnigan octapole electrospray mass spectrometer. CD spectra were recorded on a Jasco J-600 spectropolarimeter.

Site-Directed Mutagenesis. The four mutants of MIF (P1G, P1A, Y95F, and N97A) were prepared using the gene for mouse MIF cloned into a pET11b vector as the template (*7*). A *Nde*I restriction site and a *Bam*HI restriction site flank the gene. Two mutants (Y95F and N97A) were constructed using the overlap extension polymerase chain reaction (*29*). The external PCR primers were oligonucleotides 5′-GCGGATAACAATTCCCCTCT-3′ (designated primer A) and 5′-CTCAGCTTCCTTTCGGGCTT-3′ (designated primer D). Primer A corresponds to the coding sequence of a region of the pET-11b vector ∼50 bp upstream from the *Nde*I restriction site, while primer D corresponds to the complementary sequence of the pET11b vector ∼20 bp downstream from the *Bam*HI restriction site. For the Y95F mutant, the internal primers were oligonucleotides 5′-GACCGGGTCTTTATCAACTAT-3′ (designated primer C) and 5′-ATAGTTGATAAAGACCCGGTC-3′ (designated primer B). For the N97A mutant, the internal primers were oligonucleotides 5′-GTCTACATCGCCTATTACGAC-3′ (designated primer C) and 5′-GTCGTAGTAGGCGATGTAGAC-3′ (designated primer B). Primer C contains the codon for the desired mutant (underlined), and the remaining bases correspond to the coding sequence of MIF. Primer B is the complementary primer with the desired codon for the mutation underlined.

The PCRs were carried out in a Perkin-Elmer DNA Thermocycler 480 using template DNA, synthetic primers, and the PCR reagents supplied in the Perkin-Elmer Cetus

GeneAMP kit as described elsewhere (*30*). In two separate PCRs, the AB and CD fragments were generated using the plasmid pET11b as template with primers A and B in one reaction and primers C and D in a separate reaction as described (*30*). Subsequently, the mutated DNA fragment was produced by performing the PCR on a mixture of the AB and CD fragments (5 μL each) using primers A and D (*20*). The resulting, gel-purified AD fragment and the pET24a(+) vector were digested with *Bam*HI and *Nde*I restriction enzymes, purified, and ligated using T4 ligase following a previously described protocol (*26*). Aliquots of the resulting mixtures were transformed into electrocompetent *E. coli* strain DH5α cells and grown overnight on LB/Kn (100 μg/mL) plates at 37 °C (*26*). Single colonies were chosen at random and grown in liquid LB/Kn media (100 μg/mL). The newly constructed plasmid was isolated using the Wizard Plus Minipreps DNA Purification System (Promega Corp., Madison, WI) and sequenced to verify the mutation. Subsequently, the mutated plasmid was transformed into electrocompetent *E. coli* strain BL21(DE3)pLysS for protein expression (*26*).

The P1G and P1A mutants were constructed in a single PCR using two primers. One primer contained the desired mutation, and the second primer was a pET11b-vector specific primer. The mutation primer for the P1G MIF mutant was oligonucleotide 5′-AGGAGATATACATATGGGCATGTTCATC-3′, where the first 16 bases correspond to the coding sequence of the pET11b vector followed by the desired mutation (underlined) and nine bases of the MIF gene. The mutation primer for the P1A MIF mutant was oligonucleotide 5′-AGGAGATATACATATGGCCATGTTCATC-3′, where the desired mutation is underlined. The vector-specific primer was oligonucleotide 5′-CTCAGCTTCCTTTCGGGCTT-3′, which corresponds to the complementary sequence of the region ∼20 bp downstream from the *Bam*HI restriction site. The mutated fragments were treated as described above and cloned into the pET24a(+) vector.

Overexpression and Purification of the MIF Mutants. The recombinant proteins were expressed using a modification of a previously described procedure (*20*). Typically, 2 L of cell culture yields 7−8 g of cells. MIF and the N97A mutant were purified to homogeneity (>95% as judged by SDS−PAGE) using a published procedure (*20*). The P1G, P1A, and Y95F mutants were purified to homogeneity by a modification of this literature procedure (*20*). In this modification, the most active fractions from the DEAE anion-exchange column were pooled, concentrated, and passed through the DEAE anion-exchange column a second time. Typically, the yields of purified protein per liter of culture are ∼50 mg P1G, ∼20 mg P1A, ∼30 mg Y95F, and ∼30−40 mg of N97A.

Mass Spectrometry. The monomeric masses of the purified mutant proteins were determined by electrospray ionization mass spectrometry (ESI-MS). Samples for ESI-MS were analyzed in a solution of 80% (v/v) acetonitrile in water containing 0.05% TFA. The samples were prepared as previously described (*24*). Typically, each protein elutes ∼10 min after the injection. The observed monomeric molecular masses (MH^+) for MIF, P1G, P1A, Y95F, and N97A were 12 371 (calc. 12 373), 12 335 (calc. 12 333), 12 347 (calc. 12 347), 12 358 (calc. 12 357), and 12 330 (calc, 12 330) Da, respectively.

Circular Dichroism Spectroscopy. Circular dichroism spectra of the wild-type protein and the four purified mutants were measured in 20 mM Tris buffer containing 20 mM NaCl buffer (pH 7.4) at a concentration of approximately 10 μM in a CD cell with a 1.0-mm optical path length.

pH Rate Profiles for P1A and Y95F MIF Mutants. The pH dependence of the P1A- and Y95F-catalyzed ketonization of **1** to **2** was determined at 23 °C as previously described (*20*, *31*). For the P1A mutant, the dependence was determined over the pH range of 4.5−7.8, and the final concentration of enzyme was 15 μM. For the Y95F mutant, the dependence was determined over the pH range of 5.4−7.8, and the final concentration of enzyme was 0.1 μM. Above pH 7.8, the rapid rate of the base-catalyzed nonenzymatic reaction precludes an accurate measurement of the enzymatic rate of reaction. The reaction was initiated by the addition of a quantity of **1** from various stock solutions (5 mM, 10 mM, 20 mM, and 50 mM) made up in ethanol. The final concentration of **1** ranged from 10 to 150 μM. The enzyme was allowed to incubate in the assay mixture for 5 min before the addition of **1**. The reported pH is measured at the end of each assay. The initial rates were determined from plots of absorbance vs time at 288 nm, and the data were fitted as described elsewhere (*20*, *31*).

Crystallization of the Y95F Mutant. The Y95F MIF mutant was crystallized using the hanging drop vapor diffusion method. Crystals were grown at 22 °C from 10 μL drops that contained 5 μL of MIF solution (16 mg/mL in 20 mM Tris buffer, pH 7.4, containing 20 mM NaCl) and 5 μL of the precipitant solution. The precipitant solution contained 25% poly(ethylene glycol)8000 and 42 mM sodium phosphate buffer, pH 7.0. Crystals appeared overnight and grew to full size of 0.3 × 0.3 × 0.8 mm in 2−3 weeks. The space group of the crystals is $P6_3$ with one trimer per asymmetric unit and 61% solvent by volume. The unit cell parameters were $a = b = 96.16$ Å, $c = 88.52$ Å.

Data Collection. Diffraction data were collected to 2.0 Å resolution from a single crystal of MIF using an RAXIS-IV image plate detector installed on a Rigaku RU200H rotating anode X-ray generator. The generator, equipped with a nickel foil filter, was operated at 5 kW (50 kV × 100 mA). Focusing mirrors were used to produce a collimated beam width of 0.3 mm at the crystal. A sweep of 71° of diffraction data was collected as a set of 71 images of 1.0° oscillations at 25 °C. The exposure time for each image was 15 min for images 1−60 and 25 min for images 61−71 at a crystal-to-detector distance of 150 mm. The data were processed using the programs DENZO and SCALEPACK (*32*). The data set is 95.9% complete from 33.0 to 2.0 Å resolution. The crystal and data collection statistics are summarized in Table 1.

Structure Determination. The crystal structure was solved by the molecular replacement method using a 1.8 Å resolution structure of murine MIF complexed with the inhibitor as a search model (*15*). The cross-rotation and translation functions were calculated with AMORE (*33*) using data collected from 10.0 and 4.0 Å resolution. The rotation function gave a top solution with a correlation coefficient (cc) of 26.4, using a trimer as the search model. The translation function solution had a cc of 49.0 and an *R*-factor of 42.1. The translation solution was refined using

Table 1: Diffraction Data and Refinement Statistics

Diffraction Data	
space group	$P6_3$
unit cell dimensions	
a (Å)	96.16
c (Å)	88.52
R_{merge} (%)	6.8 (39.0)[a]
total observations	195 439
unique reflections	30 194
resolution range (Å)	33.0−2.0
completeness (%)	95.9 (88.5)
average $I/\sigma(I)$	12.1 (3.7)
redundancy	4.3 (3.4)
Statistics for the Refined Model[b]	
no. of protein atoms	2604
no. of water molecules	60
deviation in bond distances[c] (Å)	0.013
deviation in bond angles[c]	2.4
deviation in dihedral angles[c]	27.0
deviation in improper torsions[c]	2.77
R-factor[d]	0.191
R_{free}[d]	0.231

[a] Numbers in parentheses are the values for the highest resolution bin of the data. [b] Refinement was performed with REFMAC (*35*) and the X-PLOR package, version 3.851 (*36*). X-PLOR was used for the final stages of refinement. [c] Root-mean-square deviations from the "ideal" values in the X-PLOR protein_rep.param parameter set. [d] *R*-factor calculations are based on all data including a bulk solvent correction. A test set of 5% of the data (1509 reflections) was used for the R_{free} calculation (*41*).

the rigid body refinement function in AMORE to give a cc of 77.5 and *R*-factor of 28.2. A single trimer is found in the asymmetric unit, corresponding to a Matthews' parameter of 3.2 Å^3/Da and a calculated solvent content of 61% (*34*).

Structure Refinement. The model for the crystal structure of MIF Y95F was refined with computer-based minimization alternated with manual rebuilding. All refinement was carried out with REFMAC (*35*) and X-PLOR, version 3.851 (*36*). The maximum likelihood target function in REFMAC was used for the refinement of atom positions and individual temperature factors and for the production of σ_A-weighted $2F_o-F_c$ and F_o-F_c maps used in the manual rebuilding process (*35*, *37*). Waters were added using the automated process implemented in ARP (*38*). The maps were displayed using the graphics package O (*39*), which was also used for model rebuilding. The trimer was refined without noncrystallographic symmetry restraints because the observation-to-parameter ratio is 2.5:1 for all reflections greater than 3.0 σ. X-PLOR was used in the final refinement steps including the bulk solvent correction (*40*). The refinement statistics are summarized in Table 1.

RESULTS

Production, Expression, and Characterization of the Mutants. Four mutants (P1G, P1A, Y95F, and N97A) of MIF were constructed, expressed in *E. coli* strain BL21(DE3)-pLysS, and purified to ~95% homogeneity (as judged by SDS−PAGE) using a previously described procedure or a modification of this procedure (*20*). The DNA sequence of each mutant was confirmed by DNA sequencing. The range of overproduction (per liter of culture) varied from 20 (P1G) to 50 mg (P1A).

The purified recombinant proteins were examined by ESI-MS to determine whether the initiating methionine has been

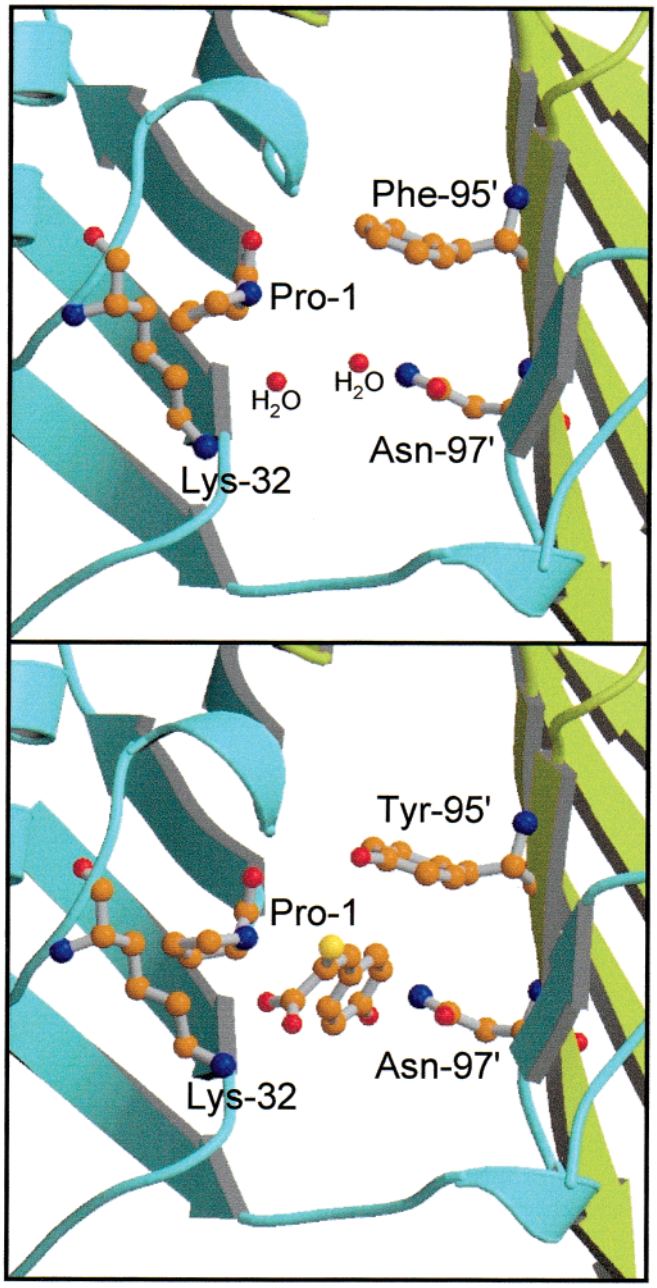

FIGURE 1: Active sites structure of the Y95F mutant and of MIF complexed with **5**. There are no significant structural differences between the two sites with the exception of the absent tyrosyl hydroxy group in the Y95F mutant. (A) Active site of the Y95F mutant at the interface of two MIF monomers. Pro-1 and Lys-32 are residues from one monomer while Phe-95′ and Asn-97′ are residues from the adjacent monomer. Two water molecules are found in the region normally occupied by a ligand. (B) Active site of MIF complexed with **5**. The molecule interacts with side chains of Pro-1, Lys-32, and Asn-97′. The figure was prepared using RASTER3D (*42*) and MOLSCRIPT (*43*).

removed. The presence of the *N*-formylmethionine substantially hinders catalysis and complicates the interpretation of kinetic studies (*21*). Mass spectral analysis of the individual proteins shows a major peak corresponding to the expected molecular mass of a 114-amino acid species. This observation indicates that each of the recombinant proteins has undergone posttranslational processing to remove the initiating *N*-formylmethionine. The structural integrity of the four mutants was also assessed by circular dichroism (CD). The CD spectra were comparable to that of the wild type indicating

Table 2: Kinetic Parameters for the PPT Activity of MIF and Mutants Using **1**[a]

enzyme	K_m (μM)	k_{cat} (s^{-1})	k_{cat}/K_m (M^{-1} s^{-1})	pK_a of Pro-1
wild type	310 ± 50	410 ± 50	1.3×10^6	5.7 ± 0.1
P1A	303 ± 70	1.7 ± 0.3	5.6×10^3	4.8 ± 0.1
P1G	107 ± 13	0.6 ± 0.1	5.6×10^3	
Y95F	112 ± 24	109 ± 14	9.7×10^5	6.3 ± 0.1
N97A	180 ± 30	660 ± 70	3.7×10^6	

[a] The steady-state kinetics parameters were determined at 23 °C. Errors are standard deviations.

Table 3: Kinetic Parameters for the PPT Activity of MIF and Mutants Using **3**[a]

enzyme	K_m (μM)	k_{cat} (s^{-1})	k_{cat}/K_m (M^{-1} s^{-1})
wild type	200 ± 24	160 ± 10	8.0×10^5
P1A	582 ± 61	4.1 ± 0.4	7.0×10^3
P1G	143 ± 25	0.8 ± 0.1	5.6×10^3
Y95F	107 ± 20	126 ± 14	1.2×10^6
N97A	110 ± 10	58 ± 4	5.3×10^5

[a] The steady-state kinetics parameters were determined in 50 mM sodium phosphate buffer (pH 6.5) at 23 °C as described elsewhere (*15*). Errors are standard deviations.

that the mutations did not result in any major conformational changes. The structural integrity of the Y95F mutant was further investigated by X-ray crystallography as described below.

Structural Characterization of Y95F MIF. The Y95F mutant of MIF was crystallized in the absence of a ligand. The structure was solved by the molecular replacement method and refined against 2.0 Å resolution data to a crystallographic *R*-factor of 19.1% and a R_{free} of 23.1%. A comparison of the active site structures for the Y95F mutant (Figure 1A) and MIF complexed with **5** (Figure 1B) shows no significant differences in the positions of the active site groups. Using the least-squares method in the program O (*39*) to superimpose the structures reveals a root-mean-square (rms) deviation of 0.28 Å for the Cα atoms and an rms deviation of 0.53 Å for all atoms. The one difference between these active sites is the presence of two water molecules in the active site of the Y95F mutant. One water molecule is located within hydrogen bonding distance of the carbonyl group of Asn-97 and is near the position occupied by the hydroxyl group of **5** in the MIF·**5** complex crystal (*15*). The other water molecule is located within hydrogen bonding distance of Pro-1 nitrogen and is near the position occupied by the carboxylate oxygen of **5** in the MIF·**5** complex crystal (*15*). The Y95F mutant of MIF did not crystallize in the presence of the competitive inhibitor **5** using the same or similar conditions to those used to produce the MIF·**5** complex crystal.

Kinetic Analysis of the P1G, P1A, Y95F, and N97A MIF Mutants. The steady-state kinetic parameters for the PPT activity of the four mutants were measured using **1** (Table 2) and **3** (Table 3) as substrates and compared to the kinetic parameters for the PPT activity of wild-type MIF. The mutation of Pro-1 to either a glycine or an alanine has little or no effect on K_m (using either **1** or **3**) but has a substantial effect on the k_{cat}. Using **1**, the k_{cat} for the P1A-catalyzed reaction is down ~240-fold, while the k_{cat} for the P1G-catalyzed reaction is down ~680-fold. The decreases in k_{cat} result in a ~230-fold reduction of k_{cat}/K_m for both mutants.[2]

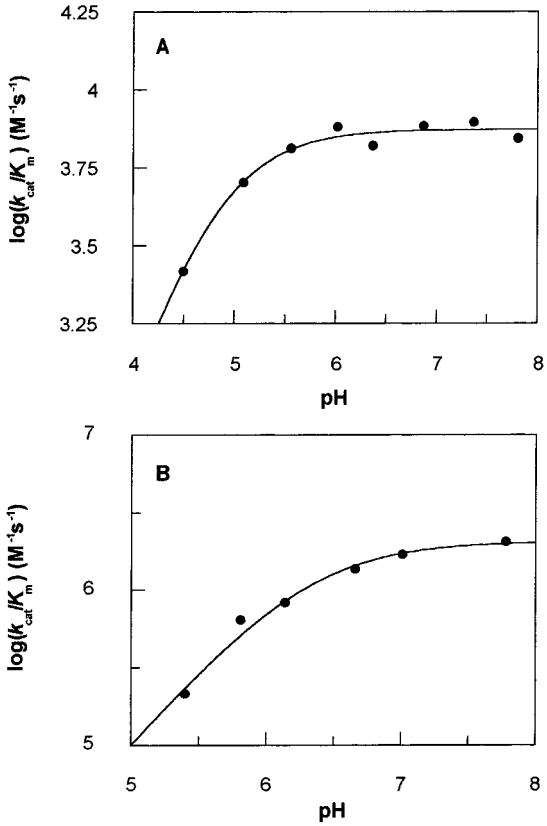

FIGURE 2: pH dependences of log(k_{cat}/K_m) are shown for the (A) P1A mutant enzyme and the (B) Y95F mutant enzyme. Curves were calculated from a nonlinear least-squares fit of the data to eq 1 as described in the text. pK_a values are reported in the text.

Using **3**, the k_{cat} for the P1A-catalyzed reaction is down ~40-fold, while the k_{cat} for the P1G-catalyzed reaction is down ~200-fold. As a result, there is a ~114-fold reduction in k_{cat}/K_m for the P1A-catalyzed reaction and a ~143-fold reduction in k_{cat}/K_m for the P1G-catalyzed reaction.

In contrast, the mutation of Tyr-95 to phenylalanine and the mutation of Asn-97 to alanine have little effect on either K_m or k_{cat}. For the Y95F mutation, there is a ~3-fold decrease in K_m and a ~4-fold decrease in k_{cat} using **1**. As a result, the k_{cat}/K_m is reduced ~1.3-fold. Using **3**, the k_{cat} decreases slightly (1.3-fold) and the K_m decreases slightly (~1.9-fold). This results in a 1.5-fold increase in k_{cat}/K_m.

pH Dependence of the PPT Activities of the P1A and Y95F MIF Mutants. The pH dependences of k_{cat} and k_{cat}/K_m for the PPT activity of P1A and Y95F MIF using **1** were determined. For both proteins, a plot of log(k_{cat}/K_m) vs pH shows a single ascending limb with a slope of 1 (Figure 2). A nonlinear least-squares fit of the pH dependence of k_{cat}/K_m to the logarithmic form of eq 1:

$$k_{cat}/K_m = (k_{cat}/K_m)^{max}/(1 + [H^+]/K_{HE}) \qquad (1)$$

where K_{HE} corresponds to the ionization constant for the free enzyme, gives the following pK_a values (*20*, *24*). For the PPT activity of P1A MIF, a pK_a value of 4.8 ± 0.1 is measured for the free enzyme (Figure 2A). For the PPT activity of Y95F MIF, a pK_a value of 6.3 ± 0.1 is measured

[2] Although the k_{cat} for the P1G-catalyzed reaction is down ~680-fold, there is a 3-fold reduction in the K_m value. As a result, the value of k_{cat}/K_m for the P1G mutant is comparable to that of the P1A mutant.

(Figure 2B). A pK_a value of 5.5 ± 0.1 has previously been reported for the PPT activity of the wild-type enzyme (*31*).

The plot of log(k_{cat}) vs pH for the PPT activity of the P1A mutant also shows a single ascending limb with a slope of 1 (data not shown). A nonlinear least-squares fit of the pH-dependence of k_{cat} to the logarithmic form of eq 2:

$$k_{cat} = (k_{cat})^{max}/(1 + [H^+]/K_{HES}) \quad (2)$$

where K_{HES} corresponds to the ionization constant for the enzyme−substrate complex, gives a pK_a value of 5.0 ± 0.5 (*20*, *24*). A pK_a value of 5.5 ± 0.2 has previously been reported for the pH-dependence of k_{cat} for the PPT activity of the wild-type protein (*31*). The plot of log(k_{cat}) vs pH for the PPT activity of the Y95F mutant shows an ascending limb over the pH range of 5.0−7.8, which does not level off. If there is a pK_a for a basic group in the enzyme−substrate complex, it must be greater than 7.8.

*Competitive Inhibition of the N97A MIF Mutant by **5***. It has previously been reported that **5** is a potent competitive inhibitor of the PPT activity of MIF with a K_i value of 2.6 ± 0.3 μM (*3*, *15*). The compound is also a competitive inhibitor of the PPT activity of N97A MIF with a K_i value of 13.1 ± 2.0 μM. The results show that replacing the asparagine with alanine results in a 5-fold decrease in the potency of **5**.

DISCUSSION

The interconversion of keto and enol isomers is a common enzymatic reaction. This reaction is frequently found as an intermediate step in a more complex enzyme-catalyzed process, but it can also be found as a separate reaction such as in the transformation catalyzed by the PPT activity of MIF (*44*). Many of these enzymatic reactions use concerted general acid-general base catalysis (*45*, *46*). In such a mechanism, protonation of the carbonyl oxygen by the general acid catalyst sufficiently reduces the pK_a of the α-proton so that the general base can readily abstract it. This mechanism can account for much of the rate acceleration observed for these enzyme-catalyzed reactions (*45*, *46*).

Pro-1 was initially implicated as the general base catalyst in the PPT-catalyzed reaction of MIF because of the protein's structural homology with 4-OT, a bacterial isomerase that uses the amino-terminal proline as the catalytic base (*16*−*19*). Subsequently, affinity labeling studies of MIF with 3-bromopyruvate (*20*), kinetic analysis (*20*), and NMR studies (*13*) confirmed this implication and further showed that Pro-1 has a pK_a of ∼5.6 so that it could reasonably function as a base under physiological conditions (*13*). Recent crystallographic and mutagenesis studies provided additional evidence to support the assigned role of Pro-1 (*15*, *21*).

In view of the literature precedence, it was anticipated that a second residue would be involved in the mechanism and function as the general acid catalyst. Two crystal structures, one of the MIF·**5** complex and one with substrate **3** bound in the active site, suggest that the only proximal residue in a position to function in such a capacity is Tyr-95 (*15*, *21*). However, these crystal structures show that Tyr-95 is not within hydrogen bonding distance of the carbonyl oxygen making it an unlikely catalyst in the absence of some movement during the reaction that brings it closer to the carbonyl oxygen.

Our experiments clearly show that Tyr-95 is not an essential residue in the tautomerization reaction because there is not a significant difference between the kinetic parameters obtained for wild type and those measured for the Y95F mutant. It is therefore doubtful that Tyr-95 moves within hydrogen bonding distance in the course of catalysis to function as a general acid catalyst. Moreover, a comparison of the active site structures for wild type and the Y95F mutant shows that no significant structural differences result from this substitution. Because the structure of the Y95F mutant is not in a complex with a ligand, two water molecules are found in the area normally occupied by a ligand. These water molecules are presumably displaced upon substrate binding making either one an unlikely general acid catalyst. Thus, in the absence of a heretofore unobserved conformational change that brings some other polar group into the active site,[3] it does not appear that a second group functions as the general acid catalyst.

One potential explanation for this observation is that the PPT activity of MIF may be responsible for a yet undiscovered physiological reaction in which Tyr-95 functions as the general acid catalyst. The only support for the existence of such a reaction is the fact that the physiological relevance for the PPT activity is not known (*13*). Although the structures of the MIF·**3** and the MIF·**5** complexes show a "snug fit" between ligand and protein (*15*, *21*) and do not suggest obvious alternative substrates, the purpose for the keto−enol tautomerization remains unknown (*13*). If the reaction does not utilize a small molecule resembling **1**−**4**, it may transform a portion of a larger compound such as the modified side chain of a protein. A possible role for Tyr-95 in such a reaction can only be addressed once a physiologically relevant substrate is identified.

A second potential explanation for the apparent absence of a general acid catalyst is that the reaction does not require one. A general acid catalyst would not be required if the pK_a of the abstracted proton were within 2−3 pK_a units of the base catalyst, Pro-1 (*45*). The pK_a of the α-proton of **2** is estimated to be ∼13−14 based on the pK_a determined for pyruvate (16.6) (*47*) and the acid strengthening effect of a phenyl substituent (∼3−4 pK_a units) (*48*). The pK_a for Pro-1 is ∼5.6 (*13*). Thus, the pK_a of the α-proton of **2** must be decreased another 7−8 pK_a units to match the pK_a of the base catalyst indicating that a general acid catalyst is required.

A third possible explanation is that PPT activity of MIF uses a mechanism in which Pro-1 function as both the general base and general acid catalysts. Accordingly, for the ketonization of **1** to **2** (or **3** to **4**), the conjugate base of Pro-1 initiates the reaction by deprotonation of the 2-hydroxy group of the enol (Scheme 2). Subsequently, the charged form of Pro-1 delivers a proton to C-3 to afford **2** (or **4**). For the enolization reaction, the charged form of Pro-1 protonates the carbonyl oxygen of **2** (or **4**), while the conjugate base abstracts the α-proton.

[3] This possibility is remote in view of the crystal structures obtained to date. The structures of the free MIF and the MIF·**5** complex are nearly identical with a root-mean-square deviation of 0.34 Å for the Cα positions (*15*). Likewise, the structures of the free MIF and the MIF·**3** complex are also nearly identical (*21*). Neither structure indicates any major conformational changes upon ligand binding (*15*, *21*).

Scheme 2

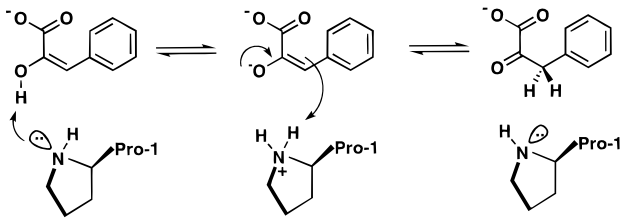

The strongest support for this mechanism comes from the observation that of all the reported mutants of active site residues, only those of Pro-1 affect catalysis. Pro-1, Tyr-95, Asn-97, and Lys-32 are found in the region assigned to the PPT activity of MIF and have been mutated to assess their role in catalysis (*15*, *21*). The results reported here clearly show that neither the Y95F mutant nor the N97A mutant has a significant effect on catalysis. The only effect of the Tyr-95 mutation appears to be a 0.6 unit increase in the pK_a of the catalytic base, while the most notable effect of the Asn-97 mutation is a decrease in the binding affinity for **5**.[4] Previous studies have shown that the primary effect of Lys-32 mutations is on the pK_a of Pro-1, indicating that the positive charge of Lys-32 is partially responsible for lowering the pK_a of Pro-1 (*31*).

In contrast to these observations, mutations of Pro-1 severely impair catalysis (*13*, *14*, *21*). The most extensively characterized P1 mutants are the P1G, P1A, and P1S mutants, which have some activity, and the P1F mutant, which has no detectable activity (*14*). Examination of the kinetic properties for the P1G, P1A, and P1S mutants shows that the major effects of replacing a rigid secondary amine (i.e., proline) with the more flexible primary amines (i.e., glycine, alanine, and serine) are on the values of k_{cat} and k_{cat}/K_m (*14*). This suggests that the decrease in catalysis for these three mutants may be due to a combination of effects including the lower basicity of the primary amine, the increased flexibility of the amine resulting in suboptimal positioning of the general base, and the slower release of product (*14*, *21*).

There are two explanations for the observation that the P1F mutant, which is isolated with a methionine-blocked amino-terminus, is inactive (*14*). The presence of the extra amino acid may push the amino-terminal group of the methionine out of the hydrophobic pocket so that it does not have a significantly low pK_a value to function as a general base (*14*, *21*). Alternately, the large phenyl side chain of the P1F mutant may limit the mobility of the amino-terminal group or completely block the active site (*14*).

The proposed mechanism for the PPT activity of MIF shares similarity with one proposed for 4-OT (*24*). 4-OT catalyzes the conversion of unconjugated α-keto acids such as 2-oxo-4-hexenedioate (**6**) to its conjugated isomer, 2-oxo-3-hexenedioate (**8**) through the dienol intermediate 2-hydroxy-2,4-hexadiene-1,6-dioate (**7**) known more commonly as 2-hydroxymuconate (Scheme 3) (*19*). The substrate for the reaction, **6**, cannot be synthesized nor isolated—it exists in rapid equilibrium with **7**. Hence, studies of 4-OT utilize the observation that **7** as well as the related dienols are partitioned to both **6** and **8** (*50*). One question that arises is how does the enzyme obtain a proton to place at C-3 (to produce **6**) or at C-5 (to generate **8**) (*24*). The proposed mechanism is that 4-OT abstracts the proton from the 2-hydroxy group of **7** and delivers it to either C-3 or to C-5 (*24*), analogous to the mechanism proposed here for the ketonization of **1** and **3**.

Scheme 3

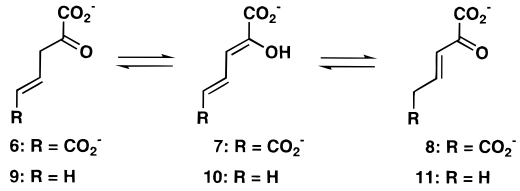

Finally, MIF, 4-OT, and CHMI are classified as members of an enzyme superfamily that may have evolved from a common ancestral protein responsible for the keto−enol tautomerization of a pyruvyl moiety (*17*, *20*). The mechanistic and structural similarities among these proteins raise questions about the extent to which they are related. One particular question is whether MIF catalyzes an isomerization reaction analogous to the reactions catalyzed by 4-OT and CHMI (*15*, *20*, *31*). 4-OT and CHMI readily partition dienols such as **7** and 2-hydroxy-2,4-pentadienoate (**10**, Scheme 3) to their respective β,γ- and α,β-unsaturated ketones (*50*). We have also shown that MIF readily converts **10** to 2-oxo-[3-D]pent-4-enoate (**9**, Scheme 3) with a high degree of stereoselectivity, in D_2O (*31*). In contrast, the MIF-catalyzed production of 2-oxo-pent-3-enoate (**11**, Scheme 3) from **10** is barely, if at all, detectable.[5] Although this result could be attributed to that fact that **10** is not a physiological substrate for MIF, our proposed mechanism suggests that MIF cannot catalyze an isomerization reaction. If Pro-1 functions as both the general acid and base catalysts in the PPT activity of MIF, then its ability to transfer a proton to C-5 to generate **11** would be limited. The limited mobility would make MIF an effective tautomerase but an ineffective isomerase. Thus, while tautomerization could be achieved using a single bifunctional group (i.e., Pro-1), isomerization requires the presence of separate general base and acid catalysts. We are currently characterizing other members of this superfamily to determine whether this observation is generally applicable.

[4] It is interesting to note that the pK_a of the enzyme−substrate complex for the Y95F mutant (pK_a > 7.8) is significantly greater than that observed for wild type (pK_a ∼ 6.2) (*20*), although the pK_a values for the free enzymes are comparable. There are several potential explanations for this observation. There may be a change in the environment of the catalytic residue in the enzyme−substrate complex for the Y95F mutant (if the pK_a value can be assigned to Pro-1), which does not occur in the wild type. The values may also be perturbed if the ratio of the nonproductive to productive ES complex is pH-dependent (*49*).

[5] S. L. Stamps and C. P. Whitman, 1999, unpublished results.

ACKNOWLEDGMENT

We are grateful to Dr. R. Bucala for providing us with the clone containing the recombinant mouse MIF. Electrospray ionization mass spectrometry was performed by the analytical instrumentation service core supported by Center Grant ES 07784.

REFERENCES

1. Knox, W. E., and Pitt, B. M. (1957) *J. Biol. Chem. 225*, 675−688.

2. Blasi, F., Fragomele, F., and Covelli, I. (1969) *J. Biol. Chem. 244*, 4864−4870.
3. Pirrung, M. C., Chen, J., Rowley, E. G., and McPhail, A. T. (1993) *J. Am. Chem. Soc. 115*, 7103−7110.
4. Shigemori, H., Sakai, N., Miyoshi, E., Shizuri, Y., and Yamamura, S., (1990) *Tetrahedron 46*, 383−394.
5. Rosengren, E., Aman, P., Thelin, S., Hansson, C., Ahlfors, S., Bjork, P., Jacobsson, L., and Rorsman, H. (1997) *FEBS Lett. 417*, 85−88.
6. Bloom, B. R., and Bennett, B. (1966) *Science 153*, 80−82.
7. Bernhagen, J., Mitchell. R. A., Calandra, T., Voelter, W., Cerami, A., and Bucala, R. (1994) *Biochemistry 33*, 14144−14155.
8. Calandra, T., Bernhagen, J., Metz, C. N., Spiegel, L. A., Bacher, M., Donnelly, T., Cerami, A., and Bucala, R. (1995) *Nature 377*, 68−71.
9. Bucala, R. (1996) *FASEB J. 10*, 1607−1613.
10. Donnelly, S. C., Haslett, C., Reid, P. T., Grant, I. A., Wallace, W. A. H., Metz, C. N., Bruce, L. J., and Bucala, R. (1997) *Nat. Med. 3*, 320−323.
11. Rice, G. C., Liittschwager, K., Metz, C., and Bucala, R. (1998) *Ann. Rep. Med. Chem. 33*, 243−252.
12. Bendrat, K., Al-Abed, Y., Callaway, D. J., Peng, T., Calandra, T., Metz, C. N., and Bucala, R. (1997) *Biochemistry 36*, 15356−15362.
13. Swope, M., Sun H.-W., Blake, P., and Lolis, E. (1998) *EMBO J. 17*, 3534−3541.
14. Hermanowski-Vosatka, A., Mundt, S. S., Ayala, J. M., Goyal, S., Hanlon, W. A., Czerwinski, R. M., Wright, S. D., and Whitman, C. P. (1999) *Biochemistry 38*, 12841−12849.
15. Taylor, A. B., Johnson, Jr., W. H., Czerwinski, R. M., Li, H.-S., Hackert, M. L., and Whitman, C. P. (1999) *Biochemistry 38*, 7444−7452.
16. Suzuki, M., Sugimoto, H., Nakagawa, A., Tanaka, I., Nishihira, J., and Sakai, M. (1996) *Nat. Struct. Biol. 3*, 259−266.
17. Murzin, A. G. (1996) *Curr. Opin. Struct. Biol. 6*, 386−394.
18. Subramanya, H. S., Roper, D. I., Dauter, Z., Dodson, E. J., Davies, G. J., Wilson, K. S., and Wigley, D. B. (1996) *Biochemistry 35*, 792−802.
19. Stivers, J. T., Abeygunawardana, C., Mildvan, A. S., Hajipour, G., Whitman, C. P., and Chen, L. H. (1996) *Biochemistry 35*, 803−813.
20. Stamps, S. L., Fitzgerald, C., and Whitman, C. P. (1998) *Biochemistry 37*, 10195−10202.
21. Lubetsky, J. B., Swope, M., Dealwis, C., Blake, P., and Lolis, E. (1999) *Biochemistry 38*, 7346−7354.
22. Harris, T. K., Cole, R. N., Comer, F. I., and Mildvan, A. S. (1998) *Biochemistry 37*, 16828−16838.
23. Taylor, A. B., Czerwinski, R. M., Johnson, Jr., W. H., Whitman, C. P., and Hackert, M. L. (1998) *Biochemistry 37*, 14692−14700.
24. Harris, T. K., Czerwinski, R. M., Johnson, Jr., W. H., Legler, P. M., Abeygunawardana, C., Massiah, M. A., Stivers, J. T., Whitman, C. P., and Mildvan, A. S. (1999) *Biochemistry 38*, 12343−12357.
25. Czerwinski, R. M., Harris, T. K., Johnson, Jr., W. H., Legler, P. M., Stivers, J. T., Mildvan, A. S., and Whitman, C. P.-(1999) *Biochemistry 38*, 12358−12366.
26. Sambrook, J., Fritsch, E. F., and Maniatis, T. (1989) *Molecular Cloning: A Laboratory Manual*, Cold Spring Harbor Laboratory, Cold Spring Harbor, NY.
27. Waddell, W. J. (1956) *J. Lab. Clin. Med. 48*, 311−314.
28. Laemmli, U. K. (1970) *Nature 227*, 680−68
29. Ho, S. N., Hunt, H. D., Horton, R. M., Pullen, J. K., and Pease, L. R. (1989) *Gene 77*, 51−59.
30. Czerwinski, R. M., Johnson, Jr., W. H., Whitman, C. P., Harris, T. K., Abeygunawardana, C., and Mildvan, A. S. (1997) *Biochemistry 36*, 14551−14560.
31. Johnson, Jr., W. H., Czerwinski, R. M., Stamps, S. L., and Whitman, C. P. (1999) *Biochemistry 38*, 16024−16033.
32. Otwinowski, Z., and Minor, W. (1996) *Methods Enzymol. 276*, 307−326.
33. Navaza, J. (1994) *Acta Crystallogr. Sect. A 50*, 157−163.
34. Matthews, B. W. (1968) *J. Mol. Biol.* 33, 491−497.
35. Murshudov, G. N., Vagin, A. A., and Dodson, E. J. (1997) *Acta Crystallogr. Sect. D 53*, 240−255.
36. Brunger, A. T., Kuriyan, J., and Karplus, M. (1987) *Science 235*, 458−460.
37. Read, R. J. (1986) *Acta Crystallogr. Sect. A 42*, 140−149.
38. Lamzin, V. S., and Wilson, K. S. (1993) *Acta Crystallogr. Sect. D 49*, 129−147.
39. Jones, A. T., Zou, J. T., Cowan, S. W., and Kjeldgaard, M. (1991) *Acta Crystallogr. Sect. A 47*, 110−119.
40. Jiang, J.-S., and Brunger, A. T. (1994) *J. Mol. Biol. 243*, 100−115.
41. Brunger, A. T. (1992) *Nature 355*, 472−474.
42. Merritt, E. A., and Bacon, D. J. (1997) *Methods Enzymol. 277*, 505−524.
43. Kraulis, P. J. (1991) *J. Appl. Crystallogr. 24*, 946−950.
44. Bugg, T. (1997) *An Introduction to Enzyme and Coenzyme Chemistry*, pp 203−205, Blackwell Science, Oxford.
45. Gerlt, J. A., and Gassman, P. G. (1992) *J. Am. Chem. Soc. 114*, 5828−5934.
46. Gerlt, J. A., and Gassman, P. G. (1993) *J. Am. Chem. Soc. 115*, 11552−11568.
47. Chiang, Y., Kresge, A. J., and Pruszynski, P. (1992) *J. Am. Chem. Soc. 114*, 3103−3107.
48. Keeffe, J. R., Kresge, A. J., and Yin, Y. (1988) *J. Am. Chem. Soc. 110*, 1982−1983.
49. Fersht, A. R. (1999) *Structure and Mechanism in Protein Science*, pp 169−190, W. H. Freeman & Co., New York.
50. Lian, H., Czerwinski, R. M., Stanley, T. M., Johnson, Jr., W. H., Watson, R. J., and Whitman, C. P. (1998) *Bioorganic Chem. 26*, 141−156.

BI000373C